Restoration and strengthening measures after a large-volume cavein occurred during Road 16 construction, Jerusalem, Israel

D. Pace, D. Paonessa JV Shapir Civil and Marine Engineering Ltd - Pizzarotti & C Spa, Petach Tikva, Israel M. Moja, C. Parisi, E.M. Pizzarotti, F. Prati Pro Iter Srl, Milan, Italy

ABSTRACT: A large-volume cave-in occurred in highway tunnel TU4, already fully excavated. The excavation of the collapsed section had been completed 7 months before in TU4 and 5 months in the adjacent TU3. Before the collapse, there had been no signs of possible ongoing criticality or instability; after their sudden first hint, in few minutes, the collapse developed with a 50 m high chimney up to the surface, forming a crater, of about 1800 m³, while the material accumulated in the tunnel had a volume of about 2600 m³ in bench. The performed preliminary investigations are reported, carried out to clarify the geological-geotechnical context and the possible causes of the collapse and to establish the best measures to be implemented to restore the tunnels. Hence, the design and the measures applied to re-excavate the TU4, to secure both tunnels and to prevent the occurrence of further collapses will be illustrated.

1 INTRODUCTION

On 2021/06/07, a large-volume cave-in occurred in highway tunnel TU4 of the Road 16 in Jerusalem – Israel. After a description of Road 16's project and of the collapse, the investigations carried out with the aim of clarifying the geological-geotechnical context and the possible causes that led to the collapse, are reported. Hence, the measures implemented to restore the tunnels under safe conditions are described: i. measures carried out immediately after the collapse; ii. treatment of the debris material inside TU4; iii. measures necessary to perform the re-excavation of the TU4; iv. injections carried out from the surface, consisting of treating the soil with the aim of filling empty cavities and recompressing the decompressed material.

2 THE ROAD 16 PROJECT

The Road 16 highway represents the new road axis of penetration into Jerusalem city center for those coming from Tel Aviv (Brunori, Moja, Pace, Paonessa, Pizzarotti 2021). As shown in

Figure 1, the project involved the construction of two double-tube tunnels, Har Nof (TU1 and TU2 - L = 1400 m)) and Yefe Nof (TU3 and TU4 - L = 1250 m), as well as two underground entry ramps in the Yefe Nof tunnel (TU11 and TU12). The construction required sequential excavation in rock of sections with variable excavation width, from a minimum of 12.5 m to a maximum of 25.0 m, with overburden varying from 140 m to few meters at the adits.

From a geological point of view, the Yefe Nof tunnels crossed two formations of rather strong dolomites and limestones with sub-horizontal stratification: Aminadav in a stretch of approximately 250 m to the West side and Kefar Shaul for the rest of the layout and, particularly, in the area of our interest. The Aminadav formation is affected by frequent karst cavities, generally

empty or filled with coarse debris, while in Kefar Shaul formation they were practically absent during the advancement.

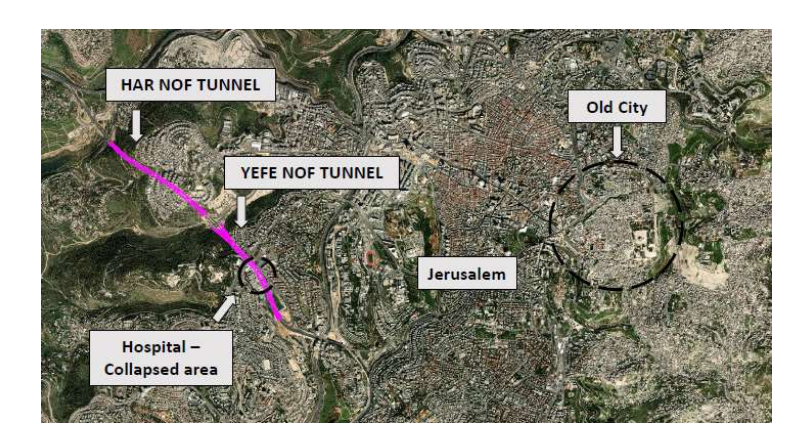


Figure 1. Road 16's plan (property of the authors).

3 COLLAPSE DESCRIPTION

The first sign of instability suddenly occurred at about 2:00 p.m. on June 7, 2021 on TU4. After a few minutes, at about 2:15 p.m., the collapse had developed up to the surface, with a 50 m high chimney, forming a crater involving a hospital parking area and swallowing several parked cars. It should be noted that on the date of the collapse there had been no signs of possible criticality or instability and that the tunnels had already been fully excavated for more than 2 months, while the excavation of the section where the collapse occurred had been completed for more than 7 months for TU4 (October 2020) and 5 months for TU3 (December 2020). At the end, the collapse involved a primary lining length of $12 \div 15$ m, made of fiber reinforced sprayed concrete, wire mesh and steel ribs (

Figure 2). During the excavation period, in the collapse area, no water flows were recorded, except for local water drips.



Figure 2. Onset of the TU4 collapse (left), formation of the surface crater (center – approximately 20 m diameter) and debris material inside the tunnel (property of the authors).

4 GEOLOGICAL-GEOTECHNICAL CONTEXT AND INVESTIGATIONS PERFORMED

To understand the phenomenon, a series of activities and investigations were carried out.

First, the geological and rock mass surveys of the tunnel face carried out during the excavation had been deeply scrutinized and four different zones from the geological and geomechanical points of view had been defined: limestone in classes Fair and Poor; limestone in classes Poor

and Very Poor; limestone in classes Very Poor, Poor and Fair with brown clay + crushed rock; brown clay + crushed rock (Extremely Poor) (Figure 3).

The mentioned rock geomechanical classes had been defined based on the Rock Mass Quality index Q (Barton) and subsequently related to the Geological Strength Index GSI (Hoek) as reported in Table 1. It should be underlined that the presence of brown clay, rather hard and dry, was not deemed to be critical during the excavation by the surveyors, the geologists and the works managers, because it didn't involve any kind of instability. Following the collapse, the stretch involved, inside the tunnel TU4 and on the surface, had been surveyed with laser scans to build a clear picture of the morphology of the collapse pile and of the surface crater.

The data acquired showed a volume of the cavity on the surface of about 1800 m³ and an accumulation of material in the tunnel of about 3800 m³, corresponding, considering an expansion factor of 1.4, to a volume of 2600 m³ in bench. This result showed that there was a strong possibility that the event could have caused the emptying of the filling of surrounding karst cavities. Considering the difference between the volume of the pile in the tunnel and that of the surface cavity, the possible volume of the voids and decompressions produced by the collapse can be estimated equal to approximately 800 m³.

In the tunnel TU4, 10 integrative convergence stations, 10 m spaced, consisting of five optical targets each, had been installed to monitor convergences and settlements and, in all the area around the cavity, a network of 63 surface benchmarks had been installed.

The following surveys were carried out to investigate the presence of possible voids and to better understand the geological-geotechnical context: i. n. 12 boreholes, 10 of them 45 m long and 2 of them 65 m long, arranged on a circle with a radius of 20 m around the surface crater and with a mutual distance of about 10 m, with SPT and Menard pressure-meter tests performed in two of them; ii. an integrated geoseismic survey combining eight seismic tomography lines, one seismic downhole test, and one seismic cross-hole test, with exploration depths ranging from 5 to 36 m, using some of the boreholes at the previous point; iii. additional geoseismic investigations from the parking lot area with GPR (Ground Penetration Radar), reaching a maximum penetration depth of 23 m; iv. n. 5 radial probe drills 12 m long executed respectively in 13 sections, 10 m spaced and distributed along the entire collapse zone, from tunnel TU3 and in 15 sections, 5 m spaced, in the areas preceding and following the collapsed zone, from tunnel TU4; v. n. 23 additional short boreholes of different lengths along the hospital perimeter.

Laboratory tests were performed with the aim of identifying the following brown clay parameters: density in dry conditions, natural water content, granulometry, suction, free swelling ratio and swelling pressure, Atterberg limits and related indexes, mineralogic composition and shear resistance in drained and undrained conditions.

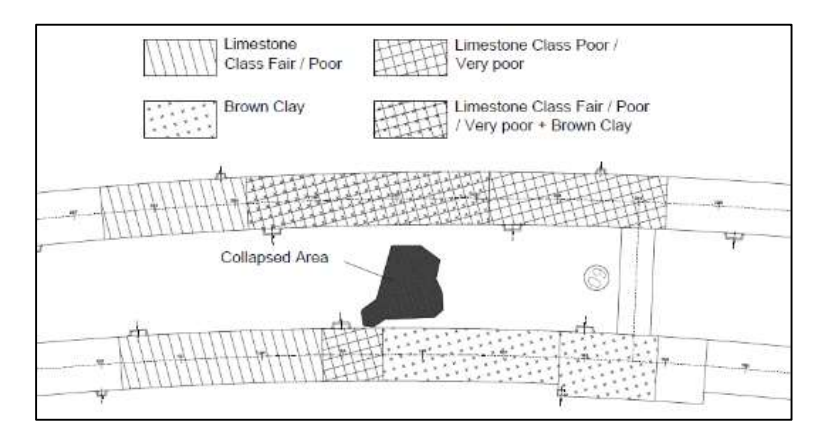


Figure 3. Geological-geomechanical reconstruction of the collapse area at tunnels' level (property of the authors).

Table 1. Geomechanical classification based on Q and GSI parameter

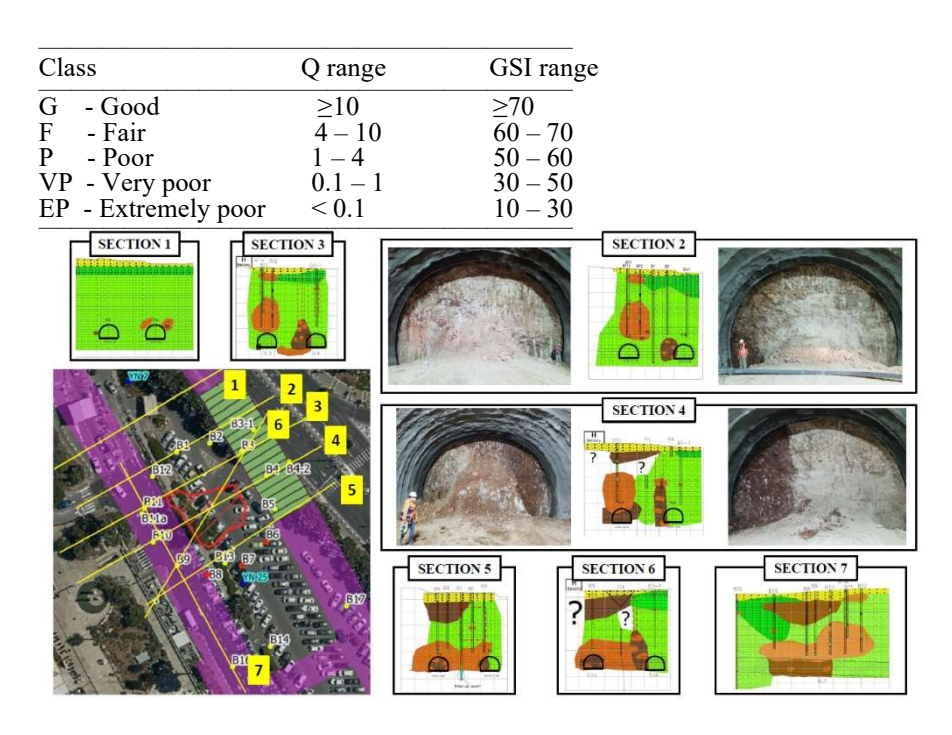


Figure 4.Geological-geomechanical reconstruction of the collapse area. From left to right: Plan view; Cross Section 1; Cross Section 3; Cross Section 2 and Cross Section 4 with related excavation fronts (TU3 on the left, TU4 on the right); Cross Section 5; Cross Section 6; Longitudinal Section 7 (property of the authors).

5 COLLAPSE'S CAUSES

Following geological-geotechnical investigations, the reliable causes triggering the collapse were identified in the presence in the area of a huge karstic sinkholes system filled by clay, showing a moderate to high swelling potential, and crushed rock and, presumably, with the presence of unfilled cavities in the dissolved limestone (

Figure 5). The karstic area, having features and dimensions completely different from the previously encountered by the excavation, was buried under the anthropic strata. Consequently, its planimetric dimension and its depth had not been duly identified by the geological survey at the design stage and were totally unexpected. It can be considered a sort of *unknown unknown* (*black swan*), whose hints were underestimated during the tunnel advancement (Soldo, Pizzarotti, Russo 2022).

Figure 6 illustrates the geological process leading to the karstic space development and the consequent tunnel collapse:

- Phase 1 Stratification of the limestone formations and geological processes such as jointing/faulting systems formation.
- Phase 2 Water flows in the cracks, dissolving the rock and creating karst cavities.
- Phase 3 Development and growth of karst cavities as a result of water flow and collapse of the rock layers above the underground voids.
- Phase 4 Collapse of the surface into the subterranean karst cavities and formation of a doline containing washed clay, crushed worn rock and boulders of rock.
- Phase 5 Clay accumulates in the doline, filling cavities and cracks.
- Phase 6 Collapse of TU4 and its filling with clay and crushed rock, and chimney/funnel formation up to the surface crater.

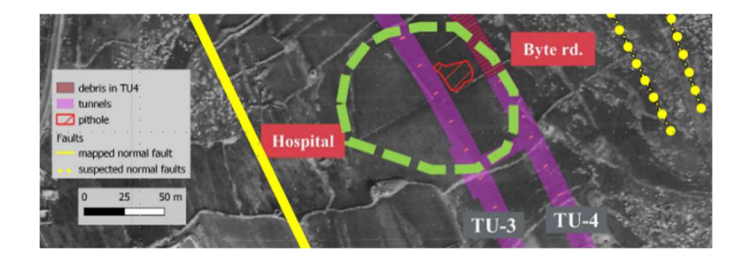


Figure 5. Air-photo from 1946 showing the pit in the striped area, a normal fault mapped in the geological map of Jerusalem in solid line, the suspected normal faults in dotted lines. The dashed thick line marks the possible doline area as recognized in the stereoscope examination (approximately 200 m diameter) (property of the authors).

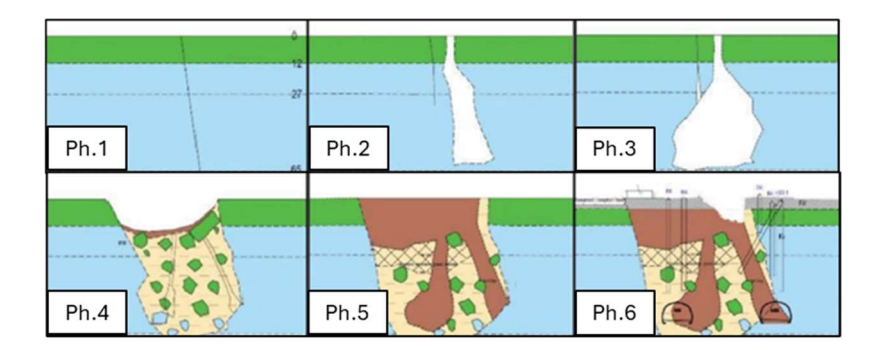


Figure 6. Geological process leading to the doline formation (phases 1 to 6) (property of the authors).

6 RECOVERING MEASURES IMPLEMENTED

6.1 Measures carried out immediately after the collapse

After the event, the first goal was to secure the tunnels along the stretches adjacent to the collapse. An additional layer of fiber-reinforced sprayed concrete was applied to the primary lining of TU3 and TU4 tunnels near the collapse. Additional material was laid to reduce the slope of the debris present in TU4 and a thick layer of sprayed concrete was applied to the surface of the debris itself and on the surrounding crown area. The unstable edges of the surface cavity were reprofiled and its walls were protected with a thick layer of fiber-reinforced sprayed concrete.

6.2 Stabilization and confinement of the debris material inside TU4

Two ramps on both sides of the collapsed material were provided and two concrete walls confining the debris pile were erected (

Figure 7). The execution of vertical and sub-vertical jet-grouting columns (nominal diameter of 80 cm, L = 6 m, array $65 \times 55 \text{ cm}$; the vertical columns were reinforced with steel pipes) at the base of the collapsed material followed (Figure 8). Then, the surface crater was filled with light concrete in successive thin layers.

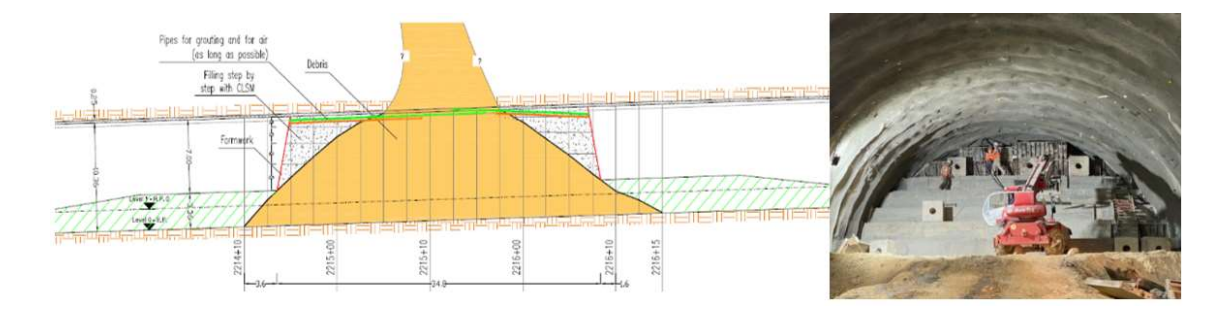


Figure 7. Stabilization of the collapsed material with ramps and CLSM walls (property of the authors).

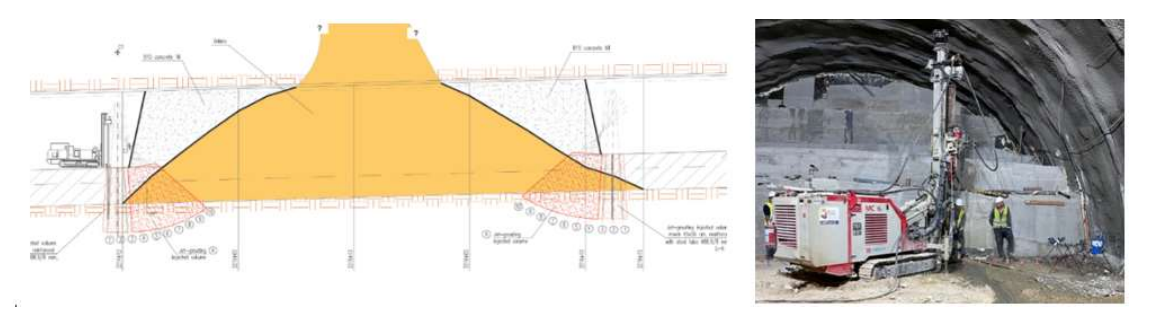


Figure 8. Vertical and sub-vertical jet-grouting columns to stabilize the base of the collapsed material (property of the authors).

6.3 Treatment of the debris material inside TU4

After the removal of the ramps and the execution of a layer of fiber-reinforced sprayed concrete on the jet-grouting wall, the injection of the collapsed material by sub-horizontal jet-grouting columns (nominal diameter of 80 cm, L=24, 18 and 12 m, array 120 x 120 cm) was carried out. The treatment of the upper part, where it was difficult to perform jet-grouting columns, was carried out with 41 cement mix injections from valved (spacing 0.5 m) PVC tubes (tube-à-manchettes - TAM) on three concentric crowns (

Figure 9). For TAM injections, the following main features were defined: cement C42.5; sheath grout: cement-water ratio (c/w) = 0.5, bentonite content 3%; strengthening cement mix: c/w = 0.5, bentonite content 1.5%; limiting volume: 450 l/m (225 l/valve - accounting for a theoretical ground absorption factor = 0.3); limiting injection pressure: 5 bar.

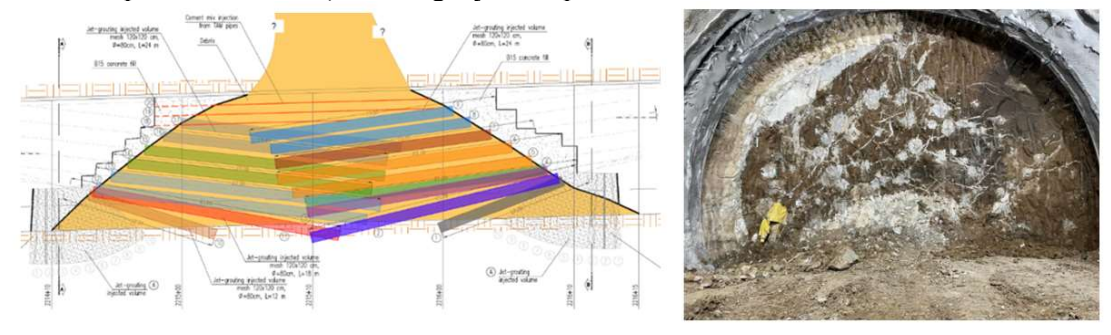


Figure 9. Treatment of the collapsed material by jet-grouting and TAM injections and their successful execution showed during the re-excavation (property of the authors).

6.4 Re-excavation of the TU4

The excavation of the collapsed material in TU4 was planned through a total of eleven sawtooth shaped fields with different lengths, excavated from both sides of the debris (Figure 10).

The strengthening measures planned consisted of 12 m-long steel pipes umbrella fields (n. 52 steel pipes coupled with two crowns of TAM injections each, 12 m-long, 33 in the upper and 34 in the lower crown. For the TAM injections on the boundary, the same properties as those used for the collapsed material were applied.

The primary support of the tunnel consisted of sprayed concrete reinforced with double steel mesh and 1 m-spaced heavy steel ribs. The excavation sequence foresaw to maintain the minimum possible distance between the front face and the casting of the final lining invert and crown.

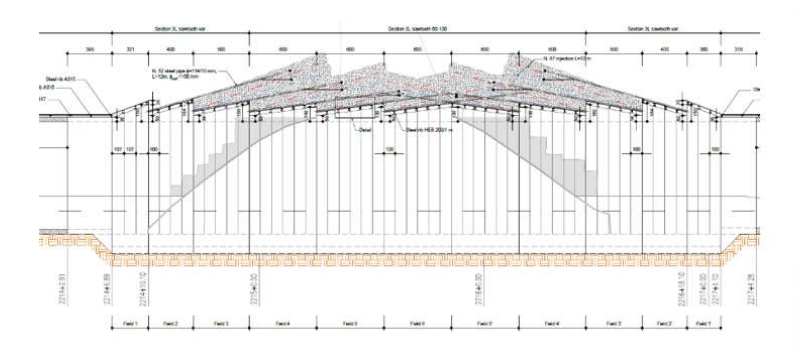


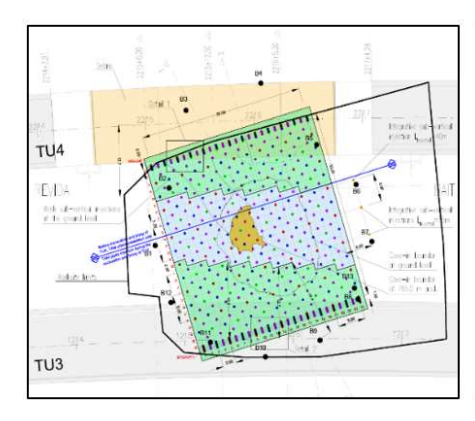


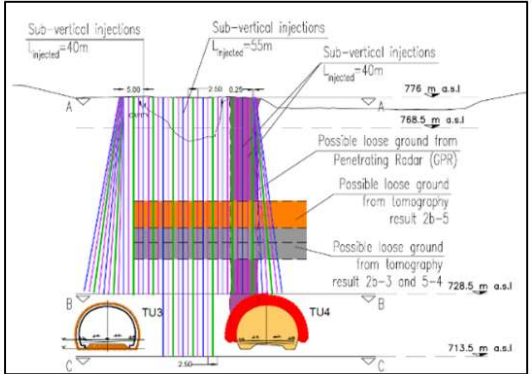
Figure 10. Measures for the re-excavation of the collapsed material and completion of the re-excavation of the TU4 tunnel (property of the authors).

6.5 TAM injections carried out from the surface

These TAM injections from the surface aimed to fill the possible empty cavities in the surrounding area, to prevent further instabilities and to recompress and stabilize the ground between the surface and the tunnels. Figure 11 shows a plan view and a cross section of the TAM injections, planned to be executed in a maximum of four stages: Stage 1 and Stage 2 having a 5 x 5 m array, Stage 3 having a 5 x 2.5 m array and Stage 4 having a 2.5 x 2.5 m array. If Stage 4 had been performed, the maximum injections density of 2.5 x 1.25 m (influence area = 3.125 m2) would had been reached. TAM injections were 40 m long (47.5 m drilling length) above TU3 and TU4 tunnels, while in the remaining area, they extend to 55 m (62.5 m drilling length); furthermore, to manage potential interference during TU4's re-excavation, specific areas were designated where injections could occur before (below the line in Figure 11 left) or after the final lining's completion (above the line).

A limiting injection volume per each valve (spacing 1 m) was set equal to 1,250 l/m (accounting for a theoretical ground absorption factor = 0.3) and a limiting injection pressure was set to 5 bar. After the completion of the Stages 1 and 2, the criterion used to proceed with the successive Stages 3 and 4 was set to a total absorption for each tube (considering both the TAM injection and the sheath grout) of 15,000 liters for 40 m injections and 20,000 liters for 55 m injections (30% of the theoretical maximum): if these injection volumes were reached or exceeded, the surrounding injection had to be carried out, otherwise they were avoided. Anyway, continuous checks were performed to ensure that anomalous absorbed volumes did not indicate the presence





of localized cavities, which were filled severally. The characteristics of the cement (C42.5) mix was also progressively improved, to reduce its fluidity: sheath grout: cement-water ratio (c/w) from 0.5 to 1.0, bentonite content from 3% to 5% and sand-cement ratio (s/c) from 0 to 1; strengthening cement mix: cement-water ratio (c/w) from 0.5 to 1.0, bentonite content from 1.5% to 3%.

Figure 11. TAM injections carried from the surface. Plan view (left) and transversal section (right) (property of the authors).

7 DESIGN ASPECTS

2D finite difference analyses (FDM, Flac software) were carried out to size the final lining still to be cast in the section where the collapse occurred. The geological simplified schematization and the geotechnical parameters adopted were inferred from all the surveys performed and from the information gathered during the drilling and injection processes. It's important to highlight the inherent limitations in conducting reliable numerical analyses due to the complex and uncertain in-situ conditions, specifically regarding the morphologies, sizes and positions of the cavities and of the decomposed soil volumes, remaining largely uncertain. The analyses were carried out in two steps. In the first step, back analyses aiming to identify the most cautious configuration, in terms of geological and geomechanical layout characterization and deconfinement rate, were performed.

Figure 12 shows the three different schematic and simplified models studied, corresponding to Cross Section 3, Cross Section 4 and Cross Section 5 of Figure 4.

In the second step, starting from the most conservative configuration defined in the previous step, the numerical analyses modelling the construction phase and the service phase were performed.

Note that, modelling both the construction and the service phases (so the long terms conditions, when all the needed TAM injections would had been completed), the geotechnical parameters were related to the natural ground without reductions, except for those consequent to the deformations associated to the collapse (say residual parameters following the back-analyses), or improvements (except for the increase of the parameters just around the perimeter of TU4, where the injections in advance had to be carried out to guarantee the stability during the re-excavation) (Table 2). In other words, the ground parameters were not enhanced beyond their state prior to the collapse but represented merely the original natural conditions.

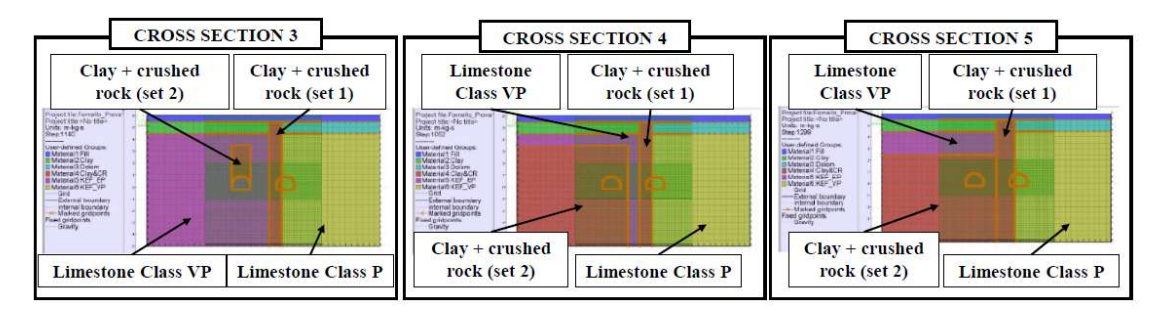


Figure 12. FDM analyses models (property of the authors).

Table 2. Geomechanical parameter: unit weight; peak friction angle; residual friction angle; peak cohesion; residual cohesion; modulus of deformation; dilation angle.

Formation	γ [kN/m ³]	φ _p [°]	φ _r [°]	c _p [kPa]	c _r [kPa]	E [MPa]	Ψ _p [°]
Clay + crushed rock (set 1)	23	20.0	20.0	50	50	200	0.0
Clay + crushed rock (set 2)	23	20.0	20.0	200	200	200	0.0
Limestone Class Poor	23	46.3	38.6	373	174	3394	5.8
Limestone Class Very Poor	23	29.9	29.0	91	84	337	0.0

8 CONCLUDING REMARKS

The difference in volume between the crater on the surface and the debris material accumulated inside the tunnel indicated a strong possibility that the event was triggered by the collapse of existing karst cavities above the tunnel crown, leading to an unacceptable stress on the tunnel lining and to its consequent catastrophic failure.

Moreover, the collapse kinematic and the fact that it happened respectively more than $5 \div 7$ months after the completion of TU3 and TU4 excavation, strongly suggests that the collapse was not closely related to the excavation itself. Instead, the tunnel excavation can be considered as the accidental victim of karst formations, an extremely unpredictable and unfavorable external condition that was difficult to detect during typical excavation surveys and finally manifested itself involving the tunnel long after construction. Even if the tunnels had not been present, a similar ground mass collapse might still have occurred, albeit with different consequences, particularly for surface infrastructure.

The execution of TAM injections, completed at the end of July 2022, was essential to address the presence of undetected cavities in the rock mass, to fill them and, also, to re-compress the loosened material around the tunnel, restoring the structural integrity of the surrounding ground mass. This approach was necessary to prevent further instabilities and to re-excavate the tunnel TU4, ending in mid-May 2022, ensuring the long-term safety of both of TU3 and TU4.

REFERENCES

Brunori G., Moja M., Pace D., Paonessa D., Pizzarotti E.M. 2021 Road 16 Highway in Jerusalem, *Gallerie e Grandi Opere Sotterranee n. 137*

Soldo L., Pizzarotti E.M., Russo G. 2022. *Handbook on Tunnels and Underground Works. Volume 1. Chapter 7*. Leiden, The Netherlands; Boca Raton, FL: CRC Press/Balkema.